Hindawi
Journal of Nanomaterials
Volume 2020, Article ID 5892506, 15 pages
https://doi.org/10.1155/2020/5892506

Research Article

Enhanced Cell Proliferation and Osteogenesis Differentiation through a Combined Treatment of Poly-L-Lysine-Coated PLGA/Graphene Oxide Hybrid Fiber Matrices and Electrical Stimulation

Jiaqi Zhu,[1,2] Zhiping Qi,[1] Changjun Zheng,[1] Pan Xue,[1] Chuan Fu,[1] Su Pan,[1] and Xiaoyu Yang[1]

[1]*Department of Orthopedic Surgery, The Second Hospital of Jilin University, Ziqiang Street No. 218, Changchun, TX 130041, China*
[2]*Department of Obstetrics and Gynecology, The Second Hospital of Jilin University, Ziqiang Street No. 218, Changchun, TX 130041, China*

Correspondence should be addressed to Su Pan; spineps@sina.com and Xiaoyu Yang; yangxiaoy@jlu.edu.cn

Received 5 November 2019; Revised 27 December 2019; Accepted 13 January 2020; Published 15 February 2020

Academic Editor: Mohammad Rahimi-Gorji

Bone tissue engineering scaffold provides an effective treatment for bone defect repair. Biodegradable bone scaffold made of various synthetic and natural materials can be used as bone substitutes and grafts for defect site, which has great potential to support bone regeneration. Regulation of cell-scaffold material interactions is an important factor for modulating the cellular activity in bone tissue engineering scaffold applications. Thus, the hydrophilic, mechanical, and chemical properties of scaffold materials directly affect the results of bone regeneration and functional recovery. In this study, a poly-L-lysine (PLL) surface-modified poly(lactic-co-glycolic acid) (PLGA)/graphene oxide (GO) (PLL-PLGA/GO) hybrid fiber matrix was fabricated for bone tissue regeneration. Characterization of the resultant hybrid fiber matrices was done using scanning electron microscopy (SEM), contact angle, and a material testing machine. According to the results obtained from the test above, the PLL-PLGA/GO hybrid fiber matrices exhibited high wettability and mechanical strength. The special surface characteristics of PLL-PLGA/GO hybrid fiber matrices were more beneficial for protein adsorption and inhibit the proliferation of pathogens. Moreover, the enhanced regulation of MC3T3-E1 cell proliferation and differentiation was observed, when the resultant hybrid fiber matrices were combined with electrical stimulation (ES). The cellular response of MC3T3-E1 cells including cell adhesion, proliferation, alkaline phosphatase (ALP) activity, calcium deposition, and osteogenesis-related gene expression was significantly enhanced with the synergistic effect of resultant hybrid fiber matrices and ES. These data indicate that the PLL-PLGA/GO hybrid fiber matrices supported the cellular response in terms of cell proliferation and osteogenesis differentiation in the presence of electrical stimulation, which could be a potential treatment for bone defect.

1. Introduction

Bone defects caused by trauma, tumor resection, or bone diseases are the common reasons of human disabilities, which often lead to serious clinical problems. At present, the transplantation of allogeneic and autologous bones remains the mainstay of treatment for bone defects [1]. However, the potential risks such as morbidity of the donor site, infection, nerve damage, and new fracture limit their usage and remain serious problems that must be resolved [2, 3]. Thus, these drawbacks also lead to the search of alternative treatment options with less additional sacrifice and more therapeutic efficiency for bone defects. In recent years, bone tissue engineering shows great potential in developing effective alternative as bone substitutes and grafts for bone defect repair. Various synthetic and natural materials, including polycaprolactone, PLGA, bioactive glasses, and chitosan, have been fabricated potential bone scaffolds that are utilized as grafts

for bone defect repair [4–7]. For PLGA materials in particular, many researchers have fabricated PLGA scaffolds for bone defect repair; they show good biocompatibility, low immunogenicity, and toxicity and are widely used in pharmaceutical and tissue engineering as an FDA certificated medical materials. However, PLGA scaffolds have hydrophobic surfaces and unsatisfactory mechanical properties, which have restricted its regenerative stimulation of large bone defects [8]. Therefore, in order to improve the bioactivity of PLGA, various chemical or physical methods have been employed, such as plasma treatment, photoreactive gelatin, poly(dopamine) coating, and nanoparticle doping [9–11].

PLL is a biocompatible cationic polymer, established as a potential compound for promoting cell adhesion, proliferation, and regeneration at the biomaterial interface [12]. In the biological medium, PLL can be as an attachment factor that enhances cell adherence due to there is an electrostatic interaction between the positive charge on the PLL molecule and the negative charge on the cell membrane. Furthermore, the PLL surface modification is simple to implement and does not require multistep polymer synthesis. Numerous studies demonstrated that PLL treatment on the surface of the scaffolds increases cell adhesion, viability, and differentiation [13, 14]. However, the PLL surface modification alone possesses limited osteoinductive abilities and cannot effectively improve the poor mechanical properties of PLGA. Therefore, to further improve the osteogenic activity of scaffold materials, the addition of some other components with good osteogenic differentiation activity to the scaffold materials might be needed. GO is a single layer of sp2-bonded carbon atoms, which has also shown great potential in biomedical applications due to its superior mechanical and biological properties [15, 16]. Compared with graphene, the presence of epoxides, carbonyls, and hydroxyls on the surface of GO makes it easily dispersed in aqueous solutions and can provide anchor sites for binding with polymers [17]. Previous studies have shown that GO can serve as an effective reinforcement filler by enhancing the network structure of the scaffolds [18, 19]. Furthermore, it has been reported that the addition of graphene and its derivatives (GO or reduced GO) could promote the cell adhesion, proliferation, and osteogenic differentiation [15, 20, 21]. More importantly, GO substrate can promote the improved of calcium deposition level and alkaline phosphatase expression [22]. This suggests that GO can be used for osteogenic stimulation of cells; it is expected to be an outstanding material as a substrate in the application of bone repair. Hence, we speculate the combination of GO and PLL surface modification can effectively improve the biological activity of PLGA.

It is known that bioelectricity plays an essential role in the functioning of all living organisms such as controlling cell behavior and promoting tissue regeneration. Thus, in the clinical treatment of bone defect, ES is a widely known adjunctive therapy used to enhance bone healing [23, 24]. It has been reported that ES to marrow mesenchymal enhanced cell proliferation compared with cells without ES [25]. Other studies also found that ES could promote mesenchymal stem cell proliferation, alkaline phosphatase (ALP) activity, and expression of vascular endothelial growth factor (VEGF) and bone morphogenetic protein-2 (BMP-2) [26]. Furthermore, previous studies found the combination of ES and biomaterials may have a better biological effect on bone repair [27, 28].

Based on the above considerations, we designed the present studies to test if combining ES and biomaterials with good bioactivity would result in optimizing bone repair effect. Firstly, PLGA blended with GO to fabricate a hybrid fiber matrices with appropriate hydrophilic and mechanical properties. Then, PLL were coated on the surface of hybrid fiber matrices to increase the number of positively charged sites for cell binding. We fully characterized the physicochemical and mechanical properties of hybrid fiber matrices using various techniques including scanning SEM, contact angle measurements, and a material testing machine. Finally, the MC3T3-E1 cells were cultured on the hybrid fiber matrices under ES to evaluate the effect of hybrid fiber matrices and ES on cell behaviors, including adhesion, proliferation, and differentiation. The preparation process and working hypothesis of the hybrid fiber matrices are schematically illustrated in Scheme 1.

2. Experimental Section

2.1. Materials. The PLGA (lactide/glycolide ratio = 75/25, Mn = 150000) was purchased from Nanjing Emperor Nano Material Co., Ltd. GO was purchased from Chengdu Organic Chemicals Co. Ltd., China (thickness: 0.55–1.2 nm; diameter: 0.5–3 μm). PLL were purchased from Sigma-Aldrich (St. Louis, US). 1,1,3,3,3-Hexafluoro-2-propanol (HFP) were purchased from Sigma, Singapore. Bovine serum albumin (BSA) was obtained from Beijing Solarbio Science & Technology Co., Ltd. The BCA protein assay kit was purchased from Sigma-Aldrich (USA). The reagents for cell experiments were purchased from Gibco (USA).

2.2. Fabrication of PLGA/GO Hybrid Fiber Matrices. PLGA/GO hybrid fiber matrices were fabricated using electrospinning technique. Briefly, for the preparation of PLGA/GO composite solution, GO nanoparticles were first doped in HFIP and homogenized for 3 h by ultrasonication to form a uniform suspension; then, PLGA was dissolved in the HFIP to obtain 20 wt% polymer solution. Finally, the GO suspension was dropped into PLGA solution and subsequently stirred at 500 rpm for 24 h, and the total solid content of GO was 2% (w/w). After that, the prepared PLGA/GO composite solution was stirred overnight at room temperature and subjected to a 3 ml syringe with 0.5 mm inner diameter needle. Finally, the mixture solution of PLGA and GO was directly electrospun onto the aluminum foil-covered collector; the electrospinning parameters were as follows: applied voltage: 40 kV; air gap distance: 20 cm; inner diameter of spinneret: 0.4 mm; and flow rate of the solution: 0.07–0.10 ml min^{-1}. The obtained PLGA/GO hybrid fiber matrices were washed three times in absolute ethanol and dried overnight under vacuum at room temperature.

2.3. Surface Modification of Hybrid Fiber Matrices with PLL. Modification of hybrid fiber matrices was performed by the

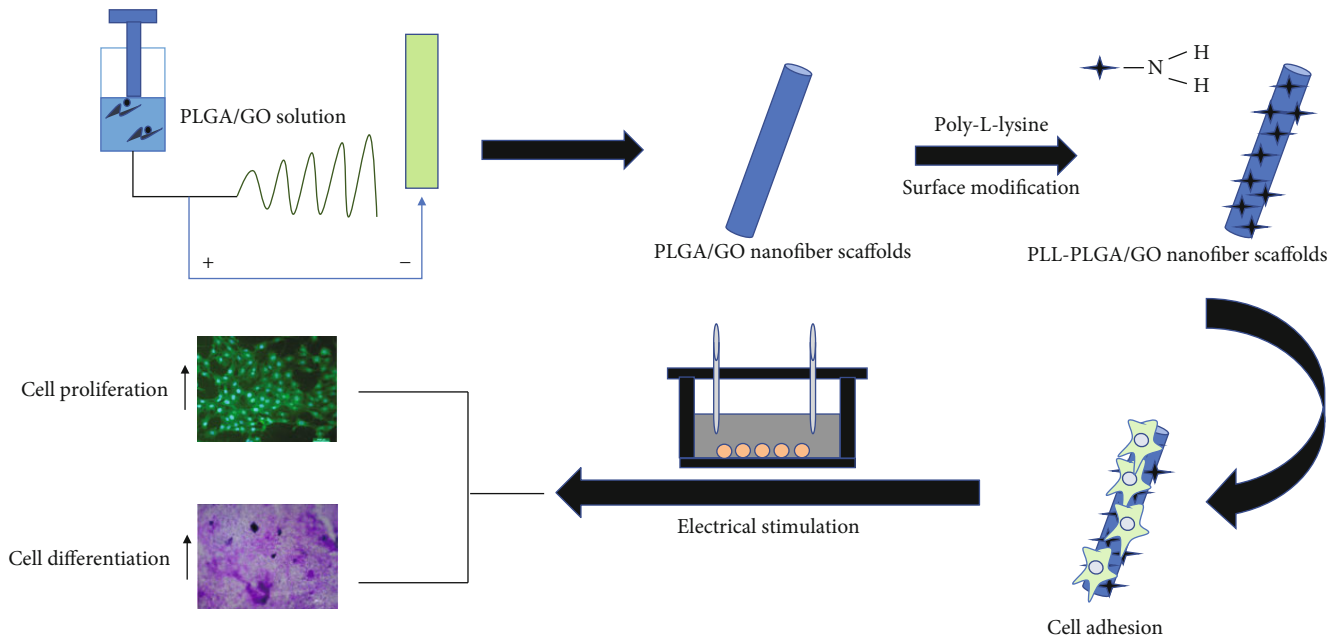

Scheme 1: Schematic illustration of PLL-PLGA/GO hybrid fiber matrix fabrication and MC3T3-E1 cell proliferation and differentiation with ES.

PLL coating method. Briefly, all hybrid fiber matrices were immersed in 5% (*w*/*v*) aqueous NaOH (Sigma) solution to obtain hydrolyzed nanofibers. Subsequently, the hybrid fiber matrices were immersed in 10 ml 0.25% (wt/vol) PLL or PLL-g-FITC solution overnight at 4°C and then rinsing in distilled water to remove the excess solution. Finally, the resulting PLL-modified PLGA/GO hybrid fiber matrices were washed by doubly distilled water and dried overnight under vacuum at room temperature.

2.4. Characterization of Hybrid Fiber Matrices. The morphologies of the hybrid fiber matrices were characterized by SEM (XL 30 ESEM-FEG, FEI) at an accelerating voltage of 15 kV. The water contact angles of the hybrid fiber matrices were measured using water contact angle analyzer (VAC2000, AST). Tensile mechanical properties of hybrid fiber matrices were determined at 20°C and 65% relative humidity with a universal mechanical testing machine (Instron 1121, UK), using nanofiber membranes with width of 10 mm, initial length of 30 mm, and thickness of 0.15–0.30 mm. Tests were performed with gauge length of 15 mm, rate of 10 mm/min, and applied load of 10 N. Tensile strength is reported as the median of 3 tests.

To directly observe the distribution of PLL on hybrid fiber matrices, FITC-labeled hybrid fiber matrices and pure hybrid fiber matrices were observed under a fluorescence microscope (TE2000-U, Nikon).

2.5. Protein Adsorption. BSA was selected as a model protein to determine the protein adsorption efficiencies of synthesized hybrid fiber matrices. The hybrid fiber matrices (PLGA, PLGA/GO, PLL-PLGA, PLL-PLGA/GO) were immerged in 10 ml BSA solution (2 mg/ml, pH 7.4) under stirring at 150 rpm for 1 h. At different time points, 3 min, 5 min, 10 min, 20 min, 40 min, and 1 h, the adsorbed BSA concentration was determined through the decrease of the concentration of BSA within the samples using BCA kit.

2.6. Antibacterial Activity Evaluation. To test the antimicrobial efficacy of the different hybrid fiber matrices, Staphylococcus aureus (S. aureus) and Escherichia coli (E. coli) were used as reference strains. S. aureus (ATCC 35696) and E. coli (ATCC 23282) were obtained from the China Center of Industrial Culture Collection. Briefly, the different hybrid fiber matrices were mixed with 1 ml of E. coli and S. aureus in LB culture medium (1×10^7 bacteria/ml), respectively. After incubation at 37°C for 3 h, bacterial suspension was collected and the wells were washed three times by 3 ml PBS. All the harvested bacteria cells were centrifuged and resuspended. Then, 30 μl of the microbial cell suspensions was spread on the nutrient agar evenly, and the tested discs were separately placed on agar for 16 h incubation at 37°C. The colonies formed on the agar plate were then observed on light microscopy. Meanwhile, to test the relative bacteria killing efficiency of different hybrid fiber matrices, the above microbial cell suspensions were incubated at 37°C for 16 h under constant shaking (120 rpm). Aliquots of 150 μl from each group were transferred to a new 96-well plate. Plates were read in a multifunctional microplate scanner (Infinite M200, TECAN) at OD 600 nm, and the results were obtained in triplicate.

2.7. Electrical Stimulation (ES) Device and Cell Culture. Cell experiments were performed by using MC3T3-E1 cells purchased from Institute of Biochemistry and Cell Biology, Shanghai Institutes for Biological Sciences, Chinese Academy of Sciences. The cells were cultured in DMEM medium supplemented with heat-inactivated 10% FBS, 10 mM HEPES,

Table 1: List of genes and primer nucleotide sequences.

Gene annotation	Forward primer sequence	Reverse primer sequence
Runx2	GCCGGGAATGATGAGAACTA	GGACCGTCCACTGTCACTTT
OPN	TCAGGACAACAACGGAAAGGG	GGAACTTGCTTGACTATCGATCAC
GAPDH	TGAACTAACACAGAGGAGGATCAG	GCTTAGGGCATGAGCTTGAC

1% penicillin, 63 mg l^{-1} penicillin, and 100 mg l^{-1} streptomycin in a humidified incubator at 37°C and 5% CO_2. The medium was changed every 2 d.

As shown in Scheme 1, a self-made ES device was designed to perform the ES experiments. In order to deliver the current to MC3T3-E1 cells, a pair of platinum electrodes were placed in the 24-well plate, and had a distance of 10 mm apart. Cells were stimulated for 2 h per day. The square wave, frequency of 200 Hz, 50% duty cycle, and electrical potential of 0.5 V were adopted in the experiment. In the following experiment, MC3T3-E1 cells were cultured under two experimental conditions: (1) hybrid fiber matrices with ES and (2) hybrid fiber matrices without ES.

2.8. Cell Adhesion and Proliferation Assays. For cell proliferation assays, MC3T3-E1 cells were seeded onto different hybrid fiber matrices with or without ES at an initial seeding density of 2×10^4 cells/ml and incubated for 3 and 7 d, respectively. At every time point, cell proliferation of MC3T3-E1 in different hybrid fiber matrices was assayed using the MTT method. Briefly, 100 μl of MTT (5 mg/ml in PBS) was added to each well, and the cells were incubated for an additional 4 h. Once completed, the medium was removed, and precipitated formazan crystals, a purple insoluble MTT product, were dissolved by 750 μl of acidified isopropanol (2 ml of 0.04 N hydrochloric acid (HCl) in 100 ml of isopropanol). The solution (150 μl) in each well was mixed and transferred to a 96-well plate, and the absorbance values at 540 nm were measured on a multifunctional microplate scanner (Tecan Infinite M200).

For cell adhesion assays, MC3T3-E1 cells were seeded onto different hybrid fiber matrices at an initial seeding density of 2×10^4 cells/ml and incubated for 3 d. The cells were washed three times with PBS, fixed with 4% paraformaldehyde (PFA) at room temperature in PBS for 10 min, dyed with 2% FITC and DAPI solution, and then washed with PBS for three times. Finally, the MC3T3-E1 morphology on different hybrid fiber matrices was observed under a fluorescence microscope (TE2000-U, Nikon).

2.9. Alkaline Phosphatase (ALP) Activity Assay. MC3T3-E1 cells were seeded on different hybrid fiber matrices with or without ES at the concentration of $2 \times l0^4$ cells/ml. After 7 and 14 days of induction, alkaline phosphatase (ALP) activity was evaluated using the p-Nitrophenyl Phosphate (pNPP) Liquid Substrate System (Sigma) according to the manufacturer's instructions. MC3T3-E1 cells were rinsed repeatedly with PBS and split by repeating freeze and thawing. Then, pNPP solution was added, and the samples were incubated in the dark for 30 min at 37°C. The spectrophotometric values at 405 nm were determined via a full wavelength reader (Infinite M200, TECAN). For ALP staining, after induction of osteoblast differentiation induction for 14 days, the cells were washed twice with PBS and were then fixed with 4% paraformaldehyde in PBS. Subsequently, ALP incubation medium was added to each well for 30 min at 37°C, and the methyl green staining solution was added to stain the cells. The ALP staining results and the cell morphology were observed under a fluorescence microscope (TE2000-U, Nikon).

2.10. Mineralization of MC3T3-E1 Cells. Calcium deposition was detected with Alizarin red S (ARS) staining of MC3T3-E1 cells after cultured on all hybrid fiber matrices. After 20 d of culture, the samples were fixed with 4% paraformaldehyde, stained with 2% ARS solution for 5 min in room temperature. In order to better observe the cell mineralization on different hybrid fiber matrices with ES or without ES, the samples were observed by a fluorescence microscope. Then, calcium quantification was measured using cetylpyridinium chloride (CPC) treatment. The absorbance of ARS at 540 nm was recorded on a multifunction microplate scanner.

2.11. Quantitative Real-Time PCR Analysis. MC3T3-E1 cells cultured on various hybrid fiber matrices with ES or without ES were incubated at 7 and 14 days. Expression of the osteogenic marker gene of MC3T3-E1 cells was quantified by real-time PCR (qRT-PCR) after RNA isolation and cDNA synthesis as per standard procedures. Total RNA was extracted by TRIzol reagent (Invitrogen) according to the manufacturer's protocol. Then, the cDNA was synthesized using a PrimeScript™ RT reagent kit (Takara Bio, Japan) according to the manufacturer's instructions. Real-time PCR was performed by Mx3005P (Stratagene, USA), and osteogenesis-related genes including anti-runt-related transcription factor 2 (Runx2) and osteopontin (OPN) were assessed. Glyceraldehyde-3-phosphate dehydrogenase (GAPDH) was used as the reference gene for the evaluation of expression of target genes (Table 1). Results were reported as relative gene expression. All experiments were done in triplicate to obtain the average data.

2.12. Statistical Analysis. Data were analyzed with Origin 8.0 (OriginLab Corporation, USA) and expressed as the mean ± standard deviation (SD). All experiments were repeated at least three times, and the statistical differences were assessed using one-way analysis of variance and a Bonferroni post hoc test. A p value of <0.05 was considered to be statistically significant.

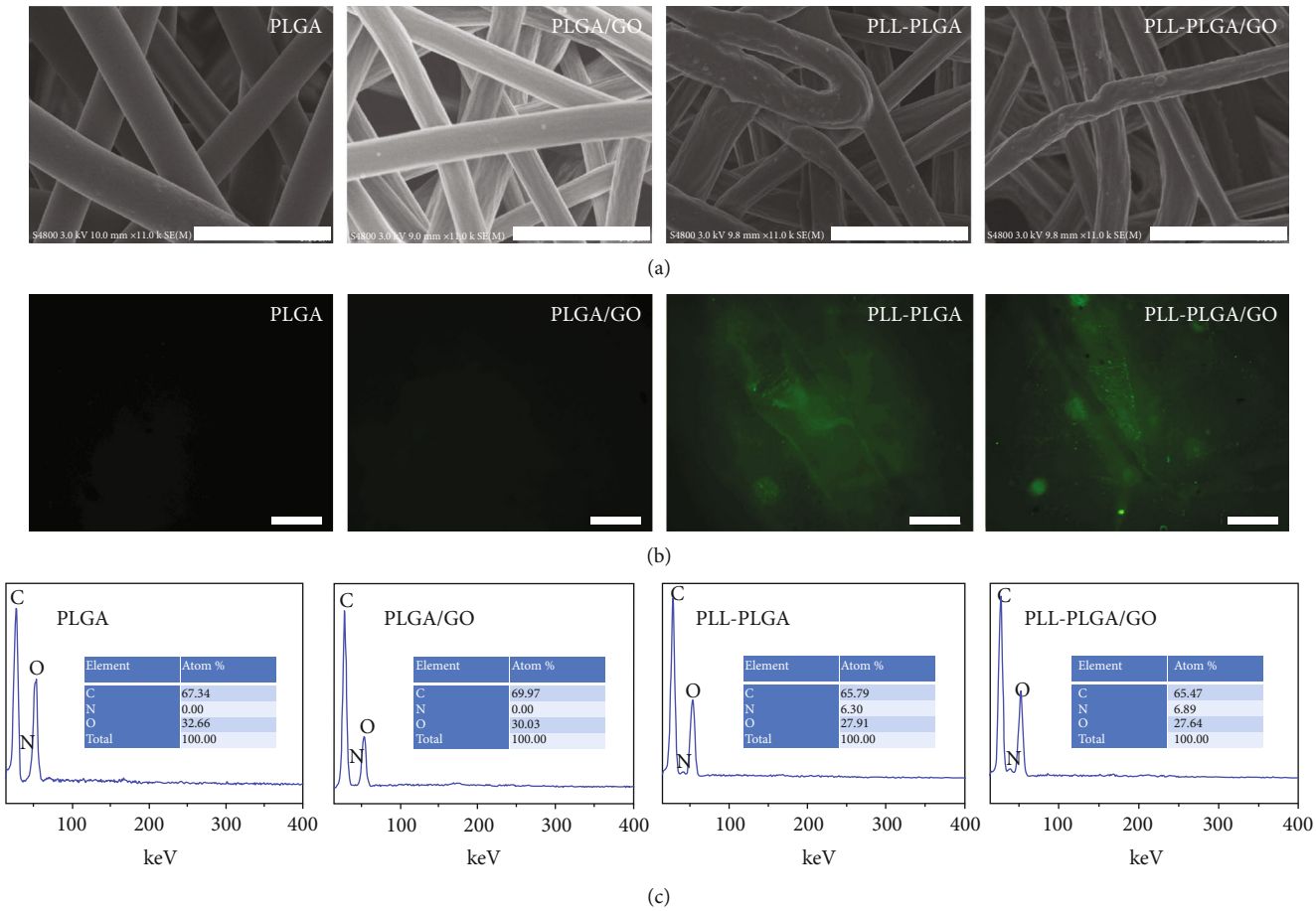

Figure 1: SEM images (a), fluorescence microscopic images (b), and EDX (c) of PLGA, PLGA/GO, PLL-PLGA, and PLL-PLGA/GO hybrid fiber matrices. Bar lengths are 5 μm (a) and 200 μm (b).

3. Results and Discussion

3.1. Characterization of PLL-PLGA/GO Hybrid Fiber Matrices. In this study, we focused on the preparation of PLL-modified PLGA/GO hybrid fiber matrices with excellent bioactivity for bone tissue regeneration. Furthermore, we systematically investigated the effect of the combined use of hybrid fiber matrices and ES on cell adhesion, proliferation, and osteogenesis differentiation. The morphology of the PLGA, PLGA/GO, PLL-PLGA, and PLL-PLGA/GO hybrid fiber matrices is shown in Figure 1(a). For PLGA hybrid fiber matrices, the surface of nanofibers is smooth and the hybrid fiber matrices have the ECM-like microstructure, which are expected to provide space gradually for supporting cell ingrowth and migration. When GO is blended with PLGA, the incorporation of GO did not seem to apparently affect the surface topography of nanofibers. Interestingly, the average diameter of PLGA was 1670 ± 187 nm, while the value of PLGA/GO nanofibers decreased to 1188 ± 173 nm, which indicated that the incorporation of GO led to the decrease of fiber diameter. This phenomenon may be due to the change in the viscosity of the solution [29]. The surface roughness of the PLGA and PLGA/GO nanofiber increased upon the surface modification with PLL. Furthermore, it is found that PLL-modified hybrid fiber matrices showed a slight decrease in fiber diameter compared to unmodified hybrid fiber matrices. We speculate that hydrolysis treatment dissolved the surface of hybrid fiber matrices, which caused the appearance change of nanofibers. The higher surface roughness of the scaffolds causes better wettability and increased the availability of medium and serum proteins, thus leading to enhanced cellular attachment and growth [30].

Whether PLL adsorbed to the surface of hybrid fiber matrices were observed via fluorescence microscopy after hybrid fiber matrices soaked in a solution of fluorescein isothiocyanate- (FITC-) labeled PLL (green). As shown in Figure 1(b), for PLL-modified hybrid fiber matrices, it was found that the PLL remained on the surface of hybrid fiber matrices after extensive washing in distilled water. However, for unmodified hybrid fiber matrices, no PLL were found on the surface of hybrid fiber matrices. Meanwhile, EDX was also applied to evaluate the changes of surface chemistry of scaffolds after being coated with PLL, and the results are shown in Figure 1(c). It was found that the major elements in the pure PLGA and PLGA/GO hybrid fiber matrices were carbon (C) and oxygen (O). After PLL surface modification, nitrogen (N) was found in the EDX spectra of hybrid fiber matrices, whereas N was not found in the EDX spectra of the two hybrid fiber matrices without PLL surface modification, which confirmed the existence of

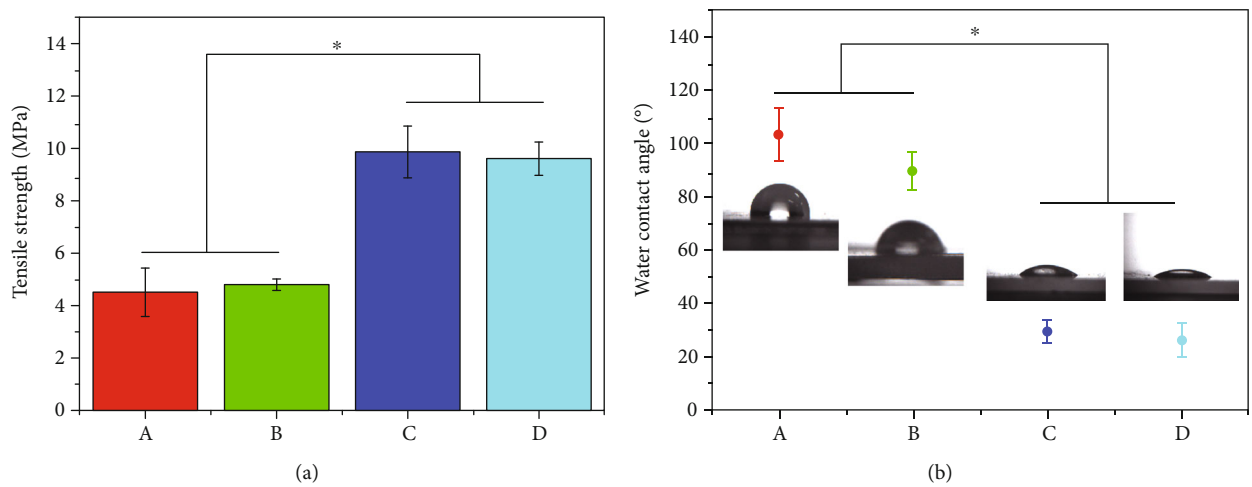

Figure 2: (a) Tensile strength of hybrid fiber matrices: PLGA (A), PLL-PLGA (B), PLGA/GO (C), and PLL-PLGA/GO (D). (b) Water contact angle of hybrid fiber matrices fabricated from PLGA (A), PLGA/GO (B), PLL-PLGA (C), and PLL-PLGA/GO (D). ∗ indicated significant difference at $p < 0.05$, $n = 3$.

PLL on the surface of scaffolds. The above results suggested that PLL accumulation was succeeded onto the surface of hybrid fiber matrices.

3.2. Surface Hydrophilicity. Generally, the hydrophilic-hydrophobic properties of scaffolds have important effects on cell behavior influencing the attachment, proliferation, migration, and differentiation of many types of cells [31]. As shown in Figure 2(b), the water contact angles of the PLGA, PLGA/GO, PLL-PLGA, and PLL-PLGA/GO hybrid fiber matrices were measured at perpendicular directions of the fibers. The PLGA hybrid fiber matrices are naturally a hydrophobic polymer showing the water contact angle of $103 \pm 9.84^{\circ}$. After blending with GO, the hybrid fiber matrices showed better hydrophilicity (the water contact angle was $89.4 \pm 7.34^{\circ}$), because of not only the hydroxyl groups but also the negatively charged groups, such as carboxylic acid groups on the GO surface. Furthermore, the alkaline solution treatment can increase the number of carboxyl groups (COOH) and negative charge on PLGA hybrid fiber matrices, which further improves the hydrophilicity of hybrid fiber matrices [32]. After PLL surface modification, PLL coating further decreased the contact angle of PLGA and PLGA/GO surfaces ($29.35 \pm 4.3^{\circ}$ for PLL-PLGA and $26.27 \pm 6.5^{\circ}$ for PLL-PLGA/GO, indicating that the hybrid fiber matrix surfaces become more hydrophilic as a result of PLL surface modification ($p < 0.05$). PLL is a positively charged polymer with a large number of amino groups, which can increase the wettability of the polymer materials [33]. On the basis of these results, it was concluded that GO and the PLL surface modification could obviously improve the surface hydrophilic property and further enhance the biological activity of hybrid fiber matrices.

3.3. Mechanical Properties. Good mechanical properties are essential for the application of scaffold materials. Figure 2(a) shows the tensile strengths of the different hybrid fiber matrices, and the tensile strengths of the PLGA, PLGA/GO, PLL-PLGA, and PLL-PLGA/GO hybrid fiber matrices were approximately 4.52 ± 0.93, 9.89 ± 1, 4.82 ± 0.23, and 9.65 ± 0.64 MPa, respectively. A significant improvement could be observed in the tensile strengths of hybrid fiber matrices with the addition of 2 wt% GO. Compare with graphene and rGO, GO has better dispersion within the polymer. Previous studies reported that the mechanical properties of polymer materials were improved by the addition of GO due to the interfacial interaction between the oxygen containing functional moieties of GO and the hydroxyl or amine groups of the polymer materials [5, 15, 34]. After PLL surface modification, it could be seen that there was no statistically significant difference in the tensile strengths of all hybrid fiber matrices before and after PLL surface modification, which indicated that the mechanical properties of hybrid fiber matrices appeared not to have been affected by the PLL surface modification. Therefore, this result suggests that the poor mechanical properties of PLGA hybrid fiber matrices can be reinforced by the impregnation of GO, and PLL surface modification has no effects on the mechanical property of hybrid fiber matrices.

3.4. Protein Adsorption Studies. When polymer material surfaces contact with biological environment, protein adsorption is the first event, which is highly related to the biocompatibility of polymer materials. In this study, we chose BSA as a model protein to determine, known to adsorb readily to surfaces and exhibiting a high abundance in blood and plasma, the protein adsorption efficiencies of different hybrid fiber matrices. As shown in Figure 3, the adsorption efficiency of BSA on different hybrid fiber matrices was examined. The BSA adsorption was determined to be 32.4 ± 1.6 mg on PLGA/GO hybrid fiber matrices, which were significantly higher than that on PLGA hybrid fiber matrices (19.6 ± 3.5 mg) ($p < 0.05$). Compared to PLGA, PLGA/GO contain oxygenous groups from GO, which introduce charged and electronegative regions to the surface and enable the formation of hydrogen bonds with proteins. At present, many studies have found that GO has strong capabilities to adsorb various proteins, including cytochrome c,

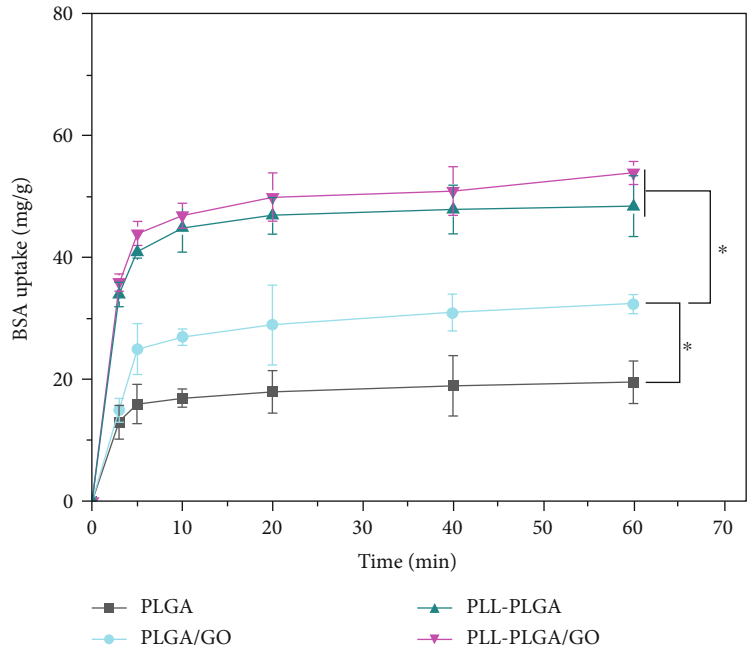

Figure 3: BSA adsorption rates of hybrid fiber matrices. BSA concentration: 2 mg/ml; pH: 7.4; ∗ indicated significant difference at $p < 0.05$, $n = 3$.

bovine serum albumin, ribonuclease A, and protein kinase A [35–37]. After PLL surface modification, PLL-PLGA and PLL-PLGA/GO hybrid fiber matrices have exhibited higher BSA adsorption capacities, nearly 2.47 and 1.66 times of adsorption rates than those of PLGA and PLGA/GO hybrid fiber matrices, respectively ($p < 0.05$). BSA has an isoelectric point of 4.7 and is negatively charged in pH 7.4 buffer. Thus, BSA was able to adsorb onto the positively charged PLL coatings via electrostatic interactions. The above results suggested that PLL-PLGA/GO have good affinity with protein and excellent biological activity for the application of bone defect repair.

3.5. Antibacterial Activity. During the treatment of bone defects, the prevention of bacterial infection is an important means to ensure bone tissue repair. At present, the most widely used method to combat bacterial infection is antibiotic therapy. However, the overuse of antibiotics can lead to bacterial resistance and reducing the treatment effectiveness [38]. Thus, manufacturing a scaffold with excellent antibacterial activity is very important to bone defect treatment. In this study, we evaluated the antibacterial performance against E. coli and S. aureus of different hybrid fiber matrices. As shown in Figure 4(a), for the PLGA samples, both E. coli and S. aureus grew very well, and PLGA hybrid fiber matrices show poor antimicrobial characteristics. When the PLGA was incorporated with 2 wt% GO, a slightly decreased number of colonies is observed from the PLGA/GO group, which shows that GO have stronger antibacterial activity against bacteria. It has been found that GO could damage the cell membrane by direct contact with the bacteria [21]. Furthermore, the unique two-dimensional structure of GO makes it easy to coat bacteria and isolate them from their surrounding environments, which can prevent the acquisition of nutrients and bacteria growth [39]. Similar results had also been reported in other graphene derivatives like rGO. After PLL surface modification, it was found that the colony number further decreased. Furthermore, among all the samples, we found that the PLL-PLGA/GO showed the strongest bacteriostatic effect and the colony number is the lowest, demonstrating that the combined use of PLL surface modification and GO has synergistic effect on the antibacterial properties of hybrid fiber matrices. Previous studies have found that PLL has good antibacterial activity on different kinds of bacteria, including S. aureus, E. coli, and Pseudomonas aeruginosa [40]. More importantly, the combined use of PLL and other antibacterial material showed improved antibacterial efficacy compared to either antibacterial material or PLL alone. As the samples of PLL-PLGA/GO hybrid fiber matrices exhibited better antibacterial activity, we chose to quantify of their relative antibacterial efficiencies. As shown in Figure 4(b), among all samples, the OD value for S. aureus and E. aureus on PLL-PLGA/GO samples is the lowest ($p < 0.05$), indicating that antibacterial efficiencies of PLL-PLGA/GO hybrid fiber matrices were more effective than other hybrid fiber matrices, which accords with the results of bacterial colony observation.

3.6. Cell Morphology and Proliferation on Different Hybrid Fiber Matrices. In our previous study, we have examined cell proliferation under ES with different frequencies and found that the 200 Hz group had the maximum cell proliferation compared to those of the other groups [41]. Therefore, we choose the frequency of 200 Hz for the subsequent cell experiments. In order to evaluate the effect of hybrid fiber matrices and ES on cell response, MC3T3-E1 cell proliferation assay of hybrid fiber matrices with ES or without ES was performed using the MTT method, and the results are shown in

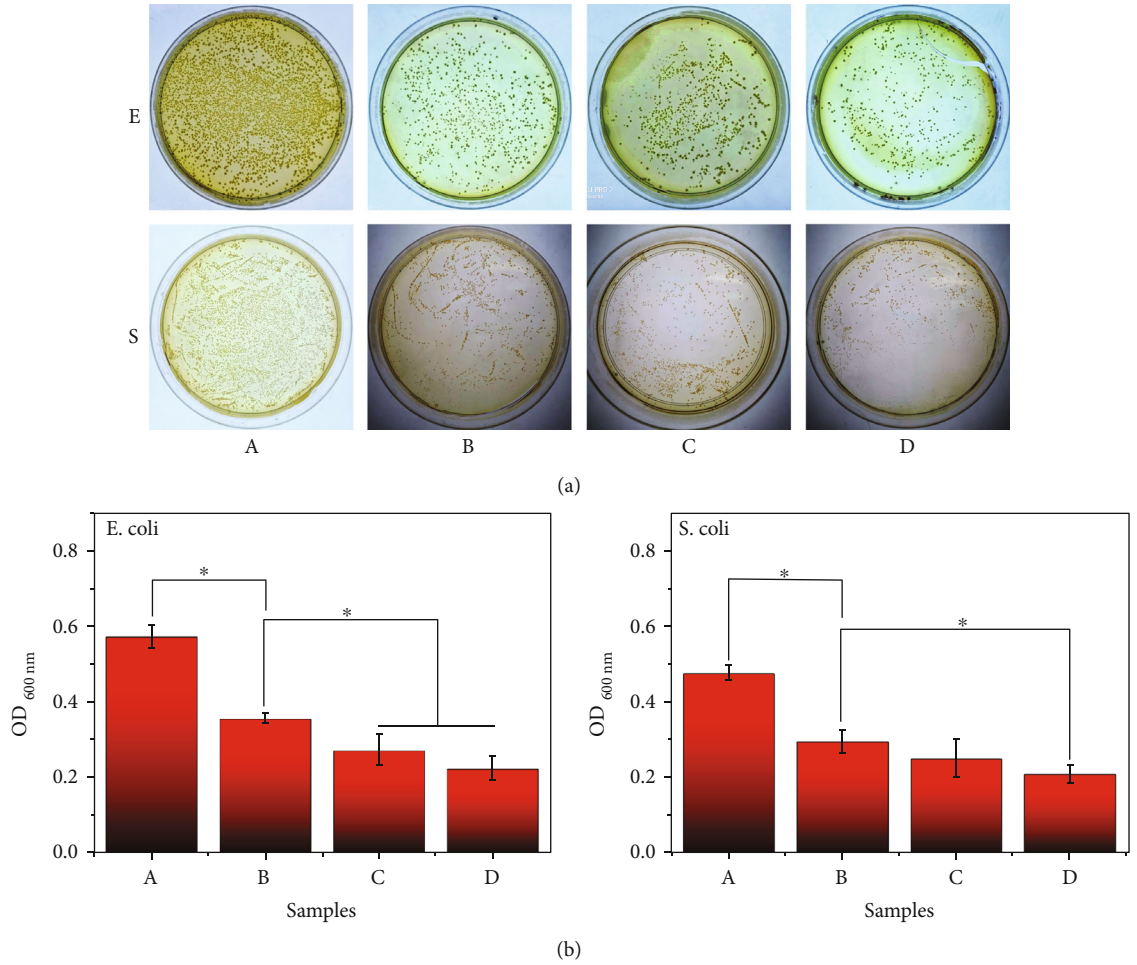

Figure 4: (a) Digital image of colony-forming unit of E. coli and S. aureus treated with (A) PLGA, (B) PLGA/GO, (C) PLL-PLGA, and (D) PLL-PLGA/GO. (b) Relatively antibacterial efficiency of E. coli and S. aureus. $*$ indicated significant difference at $p < 0.05$, $n = 3$.

Figure 5. After 3 and 7 days of the cell seeding, MC3T3-E1 cells cultured on PLGA/GO scaffolds had a better proliferation behavior than those cultured on PLGA scaffolds, which indicated that the addition of GO were beneficial for MC3T3-E1 cell proliferation. Previous studies demonstrated that GO enhances the cellular behaviors, including attachment, proliferation, and even differentiation [15, 22, 42]. After PLL surface modification, the results of cell proliferation demonstrated that MC3T3-E1 cells showed higher proliferation on the PLL-modified hybrid fiber matrices compared to unmodified hybrid fiber matrices. PLL provide abundant positive charges on the surface of hybrid fiber matrices, which can improve the interaction between cells and materials through electrostatic interactions. Furthermore, PLL surface modification can effectively improve the hydrophilicity of hybrid fiber matrices, which can provide a suitable microenvironment for the attachment and proliferation of cells. Previous studies have showed that positively charged materials have higher cell attachment, growth, and function compared to hydrophobic and negatively charged materials [43].

More importantly, compared with hybrid fiber matrices without ES, it is found that MC3T3-E1 cells showed better proliferation under ES on both day 3 and day 7, indicating that the ES also played an important role in promoting cell proliferation. Many studies have shown that ES can increase the cell proliferation rate [44]. The mechanisms of ES improved cell proliferation can be attributed to (1) increasing the secretion of growth factors, (2) activating proliferation signaling pathways, and (3) increasing intracellular calcium (Ca^{2+}). More specifically, ES can promote the release of some trophic factors from the cells, which can enhance the survival and outgrowth of cells; on the other hand, the activation of several signaling pathways by ES has been linked to an increase in cell proliferation, such as the ERK 1/2 pathway [45, 46]. Moreover, Ca^{2+} signaling can regulate various key stages of the cell cycle, including the initiation of cell proliferation via the induction of the progression from early G1 phase to S phase, followed causing the activation and expression of transcription factors [47]. This is one of the important reasons why ES can improve cell proliferation. In this study, among all hybrid fiber matrices, it is found that the cells cultured on PLL-PLGA/GO hybrid fiber matrices with ES show the highest cell proliferation rate. The above results demonstrated that the ES is used in combination with PLL-PLGA/GO hybrid fiber matrices, which have a synergistic effect in terms of cell proliferation.

As shown in Figure 6, the morphology of the MC3T3-E1 cell grown on different hybrid fiber matrices with or

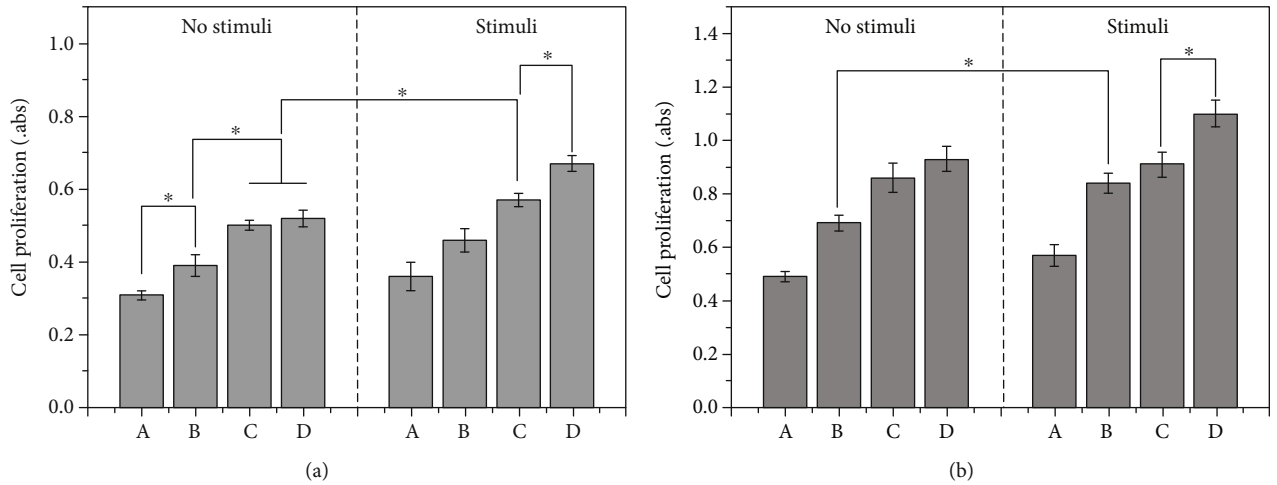

Figure 5: MC3T3-E1 cell proliferation on different hybrid fiber matrices with and without ES for (a) 3 and (b) 7 days: (A) PLGA; (B) PLGA/GO; (C) PLL-PLGA; (D) PLL-PLGA/GO. $*$ indicated significant difference at $p < 0.05$, $n = 3$.

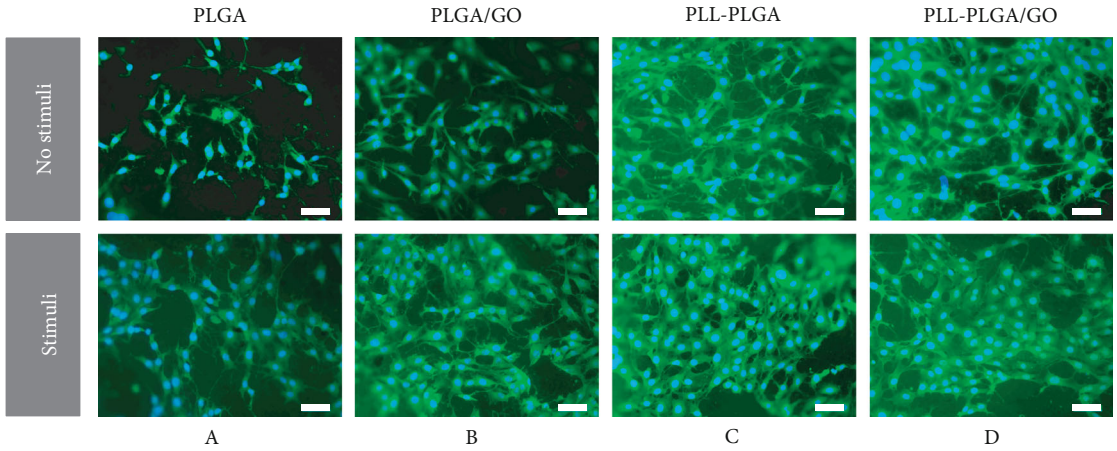

Figure 6: Morphology of MC3T3-E1 cells cultured on different hybrid fiber matrices with and without ES: (A) PLGA, (B) PLGA/GO, (C) PLL-PLGA, and (D) PLL-PLGA/GO for 3 d; scale bar lengths are 200 μm.

without ES at 3 d was further observed using a fluorescence microscope by cytoskeleton staining. Overall, the MC3T3-E1 cells maintained their normal polygonal morphology with multiple cellular projections both on all hybrid fiber matrices. After PLL surface modification, MC3T3-E1 cells exhibited a greater spread with a better cytoskeleton than those on unmodified hybrid fiber matrices. This result indicated that the cell adhesion increased after PLL surface modification due to the presence of PLL improves the surface recognition by cell. Moreover, when the MC3T3-E1 cells were employed with ES, the morphology of cells showed the more connected actin fibers and the distinct cell pseudopodium, which were beneficial to enhance the cell-cell communication. Taken together, the data clearly indicate that the cell adhesion and proliferation were significantly enhanced by the combined application of conductive hybrid fiber matrices and electrical stimulation.

3.7. Alkaline Phosphatase (ALP) Activity. ALP was one of the important early-stage osteoblastic markers, which was chosen to explore the osteoinductive activity of the different hybrid fiber matrices with or without ES. As shown in Figure 7(a), the ALP activities of cells on the PLGA/GO and PLL-PLGA/GO hybrid fiber matrices were significantly higher than those of cells on other hybrid fiber matrices, suggesting that the cell differentiation toward osteogenesis was better on the graphene oxide-impregnated hybrid fiber matrices than other hybrid fiber matrices. Furthermore, after 7 days of cell culture, it is found that there was no significant difference in ALP activity between the PLGA and PLL-PLGA hybrid fiber matrices. However, after 14 days of cell culture, the ALP activity was significantly higher in the PLL-PLGA than the PLGA hybrid fiber matrices. Previous studies have reported that lysine molecules have the potential to enhance osteoblast adhesion, possibly by imitating the structure of bovine bone protein rich in lysine to promote the attachment, growth, and differentiation of osteoblasts [48, 49]. After the cells were applied with ES, the ALP activity significantly increased on all the hybrid fiber matrices both at 7 and 14 days. More interestingly, the ALP activity in PLGA/GO

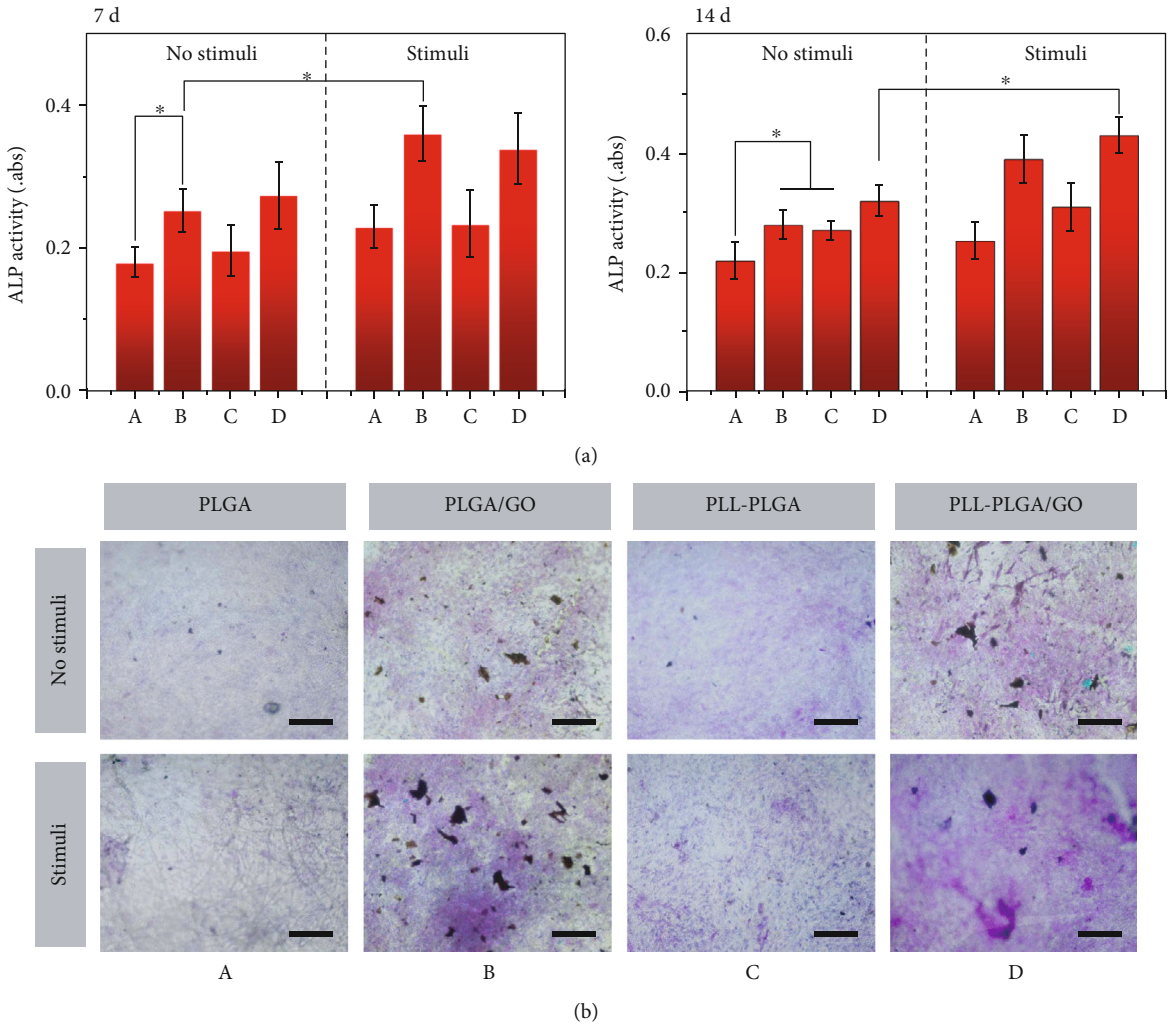

Figure 7: ALP activity (a) and staining images (b) of MC3T3-E1 cells cultured on different hybrid fiber matrices with and without ES: (A) PLGA, (B) PLGA/GO, (C) PLL-PLGA, and (D) PLL-PLGA/GO. $*$ indicated significant difference at $p < 0.05$, $n = 3$; scale bar lengths are 200 μm.

and PLL-PLGA/GO hybrid fiber matrices with ES was remarkably higher than that in other groups. Although the exact mechanism for the enhancement of ES on cell differentiation was controversial, the hypothesis of voltage-gated calcium channel had attracted particular interest. ES can adjust voltage-gated calcium channels and increase the intracellular concentration of Ca^{2+} ions, which might activate cytoskeletal calmodulin and promote cell osteogenic differentiation. Furthermore, GO can effectively improve the mechanical properties of hybrid fiber matrices, which is also an important factor affecting cell osteogenic differentiation. It was reported that the mechanical properties of scaffold materials are capable of modulating cell behaviors, such as spread area, morphology, and gene expression profile [50, 51]. For example, the MSCs on soft substrates/scaffolds had less spread, fewer stress fiber, and less proliferation rate than the MSCs on stiff substrates/scaffolds [52]. Therefore, we speculate that the mechanical properties of hybrid fiber matrices play a synergistic role with ES, which can provide a better microenvironment for cell proliferation and differentiation. To better observe the effect of different hybrid fiber matrices on cell mineralization, the dark blue staining of MC3T3-E1 cells was also observed through microscope as evidence for MC3T3-E1 cells osteogenic differentiation. As shown in Figure 7 (b), 14 days of post seeding, the dark blue staining in the cells cultured on PLGA/GO and PLL-PLGA/GO hybrid fiber matrices with ES was more intense in those cultured on other hybrid fiber matrices. The above result suggested the PLL-PLLGA/GO hybrid fiber matrices could effectively enhance the early osteogenic differentiation of cells under ES.

3.8. Cell Mineralization. Cell mineralization is the last phase of regeneration and is crucial for the final bone formation. In this study, the cell mineralization was analyzed by ARS staining, which can bind to Ca^{2+} in mineralized ECM showing bright red stains, as shown in Figure 8(b). After 20 days of cell culture, it is found that the calcium deposition was higher on the PLGA/GO than on the PLGA hybrid fiber matrices, which confirmed that the late-stage marker of osteogenic

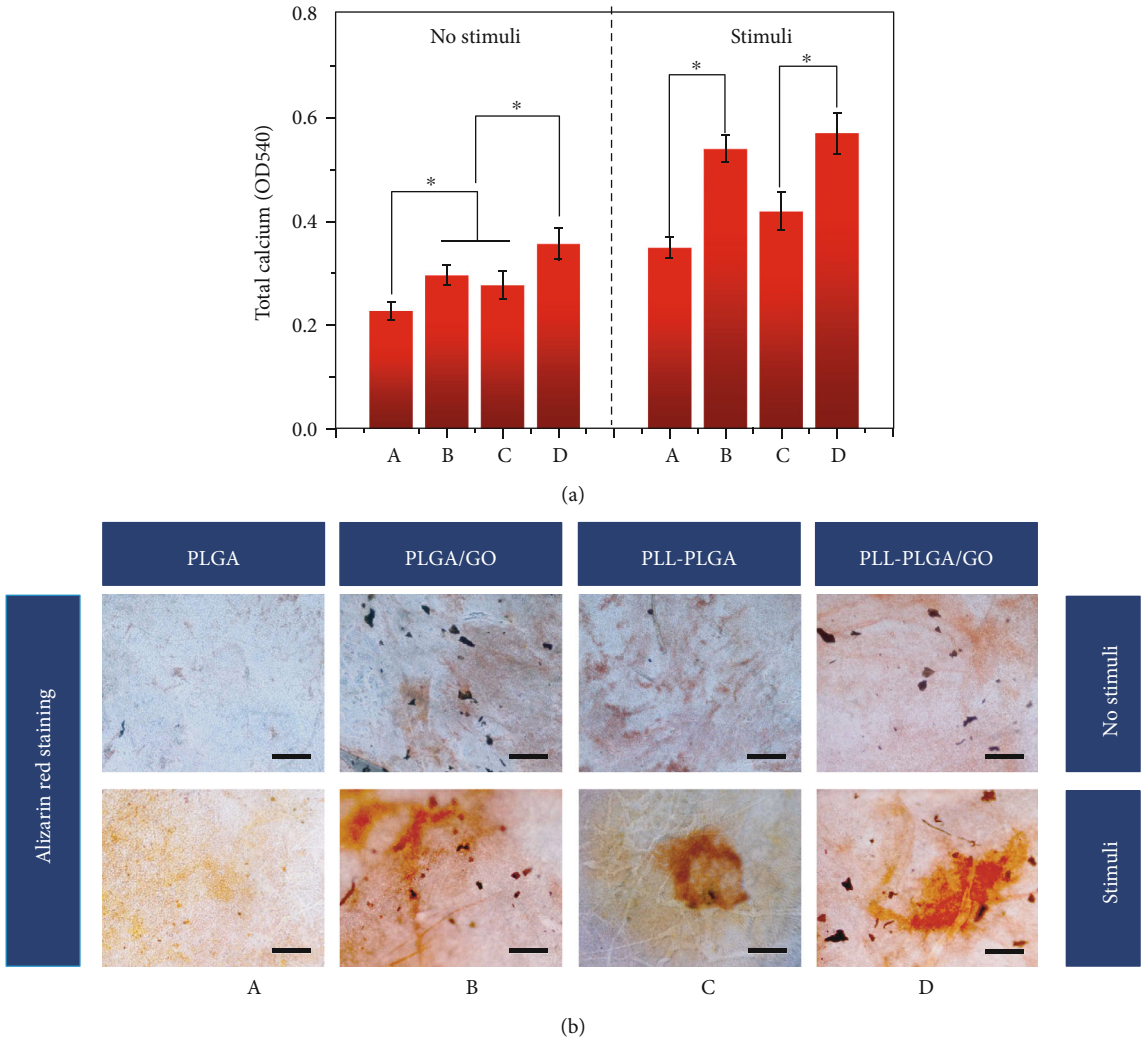

Figure 8: (a) The corresponding quantitative evaluation of calcium content mineral deposition in MC3T3-E1 cells cultured for 20 d. (b) Alizarin red staining images of MC3T3-E1 cells cultured for 20 days: (A) PLGA, (B) PLGA/GO, (C) PLL-PLGA, and (D) PLL-PLGA/GO. $*$ indicated significant difference at $p < 0.05$, $n = 3$; scale bar lengths are 200 μm.

differentiation was enhanced by the addition of GO. Interestingly, the combination of PLL surface modification and GO showed higher calcium deposition than PLL or GO alone at 20 days. The intrinsic properties of GO are thought to increase cytoskeleton tension, thus guiding cell behavior such as cell proliferation, osteogenesis differentiation, and mineralization. More importantly, due to hydrogen bonding and electrostatic interactions, graphene allows the noncovalent binding of proteins and osteogenic inducers on its surface, which can accelerate cell mineralization process. In addition, for hydroxyapatite formation, many studies have found that the poly(amino acids) such as PBLG and PLL show high calcium binding affinity, which could induce osteoblast differentiation and new bone formation [53]. Our result show that the combination of PLL surface modification and GO had a synergistic effect in terms of cell mineralization. After the cells were applied with ES, the calcium deposition of the cell was greater than that of the cells without ES at the same time. Previous studies have found that ES can activate voltage-gated Ca^{2+} channels on cell membranes which can increase the intracellular Ca^{2+} ion concentration [54]. Moreover, the Ca^{2+} ions enriched around cells might also have some contribution to favor the ion transporting into cells. And thus, these changes would induce the intracellular Ca2+ ion oscillation in cells and activate the downstream signaling pathway to promote their cell mineralization. Furthermore, consistent with ALP results, after the cells were applied with ES, the PLGA/GO and PLL-PLGA/GO hybrid fiber matrices group exhibited the largest and most calcium deposition, which further conformed the additive effect of ES and PLL-PLGA/GO hybrid fiber matrices on cell osteogenic differentiation. Thereby, PLL-PLGA/GO hybrid fiber matrices possessed good bioactivity, especially, in combination with ES, which was envisioned able to effectively promote cell osteogenesis differentiation.

The assessment of quantitative cell mineralization was performed by extracting ARS with 10% CPC. As shown in Figure 8(a), after 20 days of culture, the total calcium content

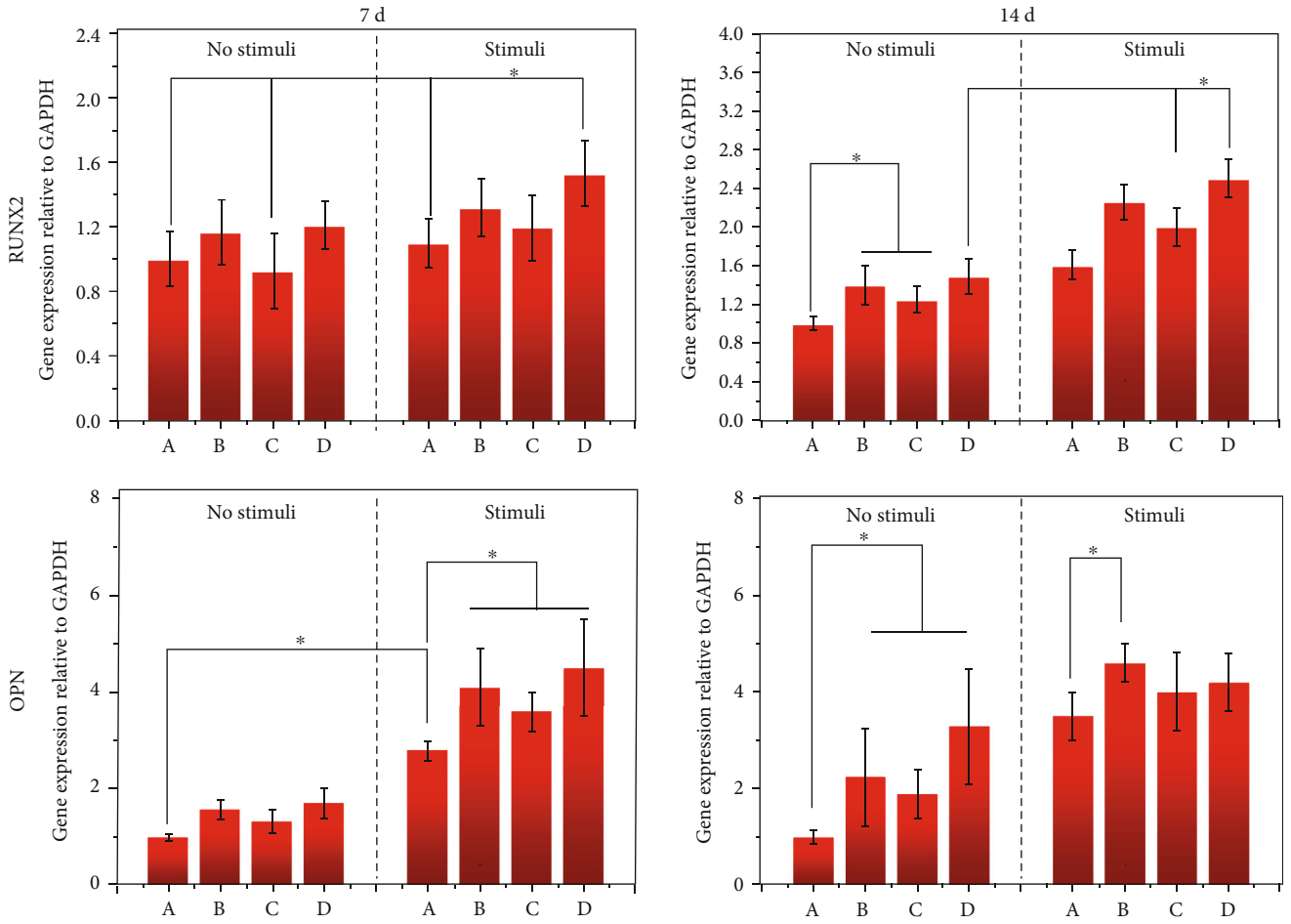

Figure 9: The qRT-PCR analysis for Runx2 and OPN expression by MC3T3-E1 cells cultured on (A) PLGA, (B) PLGA/GO, (C) PLL-PLGA, and (D) PLL-PLGA/GO hybrid fiber matrices with or without ES for 7 and 14 d. ∗ indicates significant differences ($p < 0.05$).

in PLL-PLGA/GO hybrid fiber matrices was significantly higher than that in PLGA/GO and PLL-PLGA hybrid fiber matrices. After the cells were applied with ES, the highest calcium content in deposited minerals was still observed with the PLGA/GO and PLL-PLGA/GO hybrid fiber matrices. The above result suggests that ES can effectively enhance the effect of PLL-PLGA/GO hybrid fiber matrices on the calcium mineralization of MC3T3-E1 cells.

3.9. Bone-Related Gene and Protein Expression. Some key cytokines and functional proteins such as Runx2 and OPN will be expressed regularly during the osteoblastic differentiation [55]. The Runx 2 is expressed at the early stage of differentiation. OPN expression could be observed during middle/late differentiation. As shown in Figure 9, the expression of Runx 2 was obviously upregulated on the PLGA/GO and PLL-PLGA/GO hybrid fiber matrices. However, compared with PLGA hybrid fiber matrices, Runx2 expression in PLL-PLGA group was no significant difference was observed at 7 d, and significant difference was only observed at 14 d. The above results demonstrated that PLL surface modification has less effect on the early osteogenic differentiation of cell compared with GO. For the expression of OPN, compared with PLGA hybrid fiber matrices, higher expression levels of gene were observed in PLGA/GO, PLL-PLGA, and PLL-PLGA/GO hybrid fiber matrices until 14 d. Furthermore, the expression levels of OPN in the PLL-PLGA/GO hybrid fiber matrices were obviously higher than those in PLGA/GO and PLL-PLGA hybrid fiber matrices alone. This result further demonstrated that the combination of GO and PLL surface modification had a synergistic effect in terms of osteogenic induction. When the MC3T3-E1 cells were cultured on all the hybrid fiber matrices with ES, the expression of Runx 2 and OPN was further enhanced on all hybrid fiber matrices, indicating that ES could enhance the cell osteogenic differentiation. In particular, OPN was upregulated to nearly 3-fold at 7 days, indicating that ES can result in higher increases in OPN expression. Among all samples, the highest expression level of Runx 2 and OPN was occurred in PLGA/GO and PLL-PLGA/GO hybrid fiber matrices with ES, demonstrating that the cell osteogenesis differentiation was significantly enhanced by the combined application of PLL-PLGA/GO hybrid fiber matrices and electrical stimulation. The results of bone-related genes expression showed the same trends as observed from ALP activity and cell mineralization, indicating that the PLL-PLGA/GO hybrid fiber

matrices alone could promote cell osteogenesis differentiation and the impacts and can further enhance if the cells were applied with ES.

Bone defects, caused by bone degenerative disorders, physical trauma, and cancer, were in high demand for bone grafts. In recent years, with the development of biomaterials science, a promising strategy for achieving bone tissue repair by degradable material with excellent biological activity is a very effective technique in the biomedical area. In this process, the structural characteristics of biomaterials are important for bone tissue repair, such as hydrophilicity, protein adsorption, and mechanical properties because the hybrid fiber matrices are highly porous and have a high specific surface area and ECM-like nanotopography. Thus, in this study, PLGA hybrid fiber matrices were fabricated by electrospinning. At the same time, in order to further improve the biological properties of hybrid fiber matrices, the GO and PLL surface modification was utilized to improve the biocompatibility of the PLGA hybrid fiber matrices. Previous studies have demonstrated that GO can effectively improve the mechanical properties, biocompatibility, and osteoinductive ability of the PLGA materials [5, 15]. Furthermore, because of the positive interaction between the positive charge on the PLL surface and the negative charge on the cell membrane surface, PLL surface modification can improve the affinity between materials and cells. The results of this study showed that the mechanical strength, protein adsorption, and hydrophilicity of the hybrid fiber matrices were increased by GO and PLL surface modification (Figures 2 and 3). PLL-PLGA/GO hybrid fiber matrices could effectively enhance cell adhesion, proliferation, and osteogenic differentiation (Figures 6, 7, 8, and 9). More importantly, GO and PLL surface modification showed an additive effect in improving the bioactivity of hybrid fiber matrices.

Bioelectricity plays an essential role in the functioning of all living organisms, which can control cellular functions. Thus, electrical stimulation is a widely known adjunctive therapy used to enhance bone healing. More importantly, applying ES combined with composite biomaterials that have excellent biocompatibility will further enhance ES's biological effects, which have great potential in bone defect repair [56]. For the above purpose, in this study, the effect of PLL-PLGA/GO hybrid fiber matrices under ES conditions on MC3T3-E1 cells growth and osteogenesis differentiation was systemically studied. The combination of electrical stimulation and biomaterials can maximize the speed of bone repair. In summary, the gained cellular response results indicated that the combination of electrical stimulation and PLL-PLGA/GO hybrid fiber matrices could offer two aspects to mainly influence MC3T3-E1 cells growth and osteogenesis differentiation. First, the positively charged surface, excellent hydrophilicity, protein adsorption, and mechanical properties provide a better cellular microenvironment for cell growth and osteogenesis differentiation, which is the key to bone regeneration. Second, the synergistic effect of biomaterials combined with ES could enhance the extracellular signal conduction and improve the bone conductivity. Thus, it is expected that the combination of obtained PLL-PLGA/GO hybrid fiber matrices and ES will have a broad application in the bone defect repair field. In the future, we will further investigate how these hybrid fiber matrices together with electrical stimulation modulate the intracellular cell signaling pathways to control the cell proliferation and osteogenesis differentiation.

4. Conclusions

In this study, the PLGA/GO hybrid fiber matrices were fabricated by electrospinning, and the surface of hybrid fiber matrices was further coated with PLL to improve the hydrophilicity and biocompatibility. The obtained hybrid fiber matrices have appropriate surface morphology and properties, which can meet the needs of bone tissue regeneration. In vitro MC3T3-E1 cell culture revealed better cell proliferation and differentiation on the PLL-PLGA/GO hybrid fiber matrices, and thus, they might have direct applications as bone grafts. Especially, in an electrically stimulated environment, the obtained hybrid fiber matrices with ES can further improve cell adhesion, proliferation, and osteogenesis differentiation, which were proved by MTT assay, ALP activity, calcium deposition, and osteogenic relative gene expressions. Thus, it is expected that the combination of PLL-PLGA/GO-hybrid fiber matrices and ES will have a broad application in the bone defect repair field.

Data Availability

The chart data used to support the findings of this study are included within the article.

Conflicts of Interest

The authors declare no competing financial interests and nonfinancial interests.

Authors' Contributions

Jiaqi Zhu and Zhiping Qi contributed equally to this work.

Acknowledgments

This study was supported by the by the National Natural Science Foundation of China, No. 31572217.

Supplementary Materials

Figure S1: TEM images of GO nanoparticles. *(Supplementary Materials)*

References

[1] S. L. Wu, X. M. Liu, K. W. K. Yeung, C. S. Liu, and X. J. Yang, "Biomimetic porous scaffolds for bone tissue engineering," *Materials Science and Engineering: R: Reports*, vol. 80, pp. 1–36, 2014.

[2] P. X. Ma, R. Y. Zhang, G. Z. Xiao, and R. Franceschi, "Engineering new bone tissue in vitro on highly porous poly(alpha-hydroxyl acids)/hydroxyapatite composite scaffolds," *Journal of Biomedical Materials Research*, vol. 54, no. 2, pp. 284–293, 2001.

[3] H. Shen, X. X. Hu, F. Yang, J. Z. Bei, and S. G. Wang, "An injectable scaffold: rhBMP-2-loaded poly(lactide-co-glycolide)/hydroxyapatite composite microspheres," *Acta Biomaterialia*, vol. 6, no. 2, pp. 455–465, 2010.

[4] Y. M. Hwang, C. T. Pan, Y. M. Lin et al., "Preparation of biodegradable polycaprolactone microcarriers with doxorubicin hydrochloride by ultrasonic-assisted emulsification technology," *Sensors and Materials*, vol. 31, no. 2, pp. 301–310, 2019.

[5] X. S. Ren, Q. Y. Liu, S. Zheng et al., "Synergistic delivery of bFGF and BMP-2 from poly(l-lactic-co-glycolic acid)/graphene oxide/hydroxyapatite nanofibre scaffolds for bone tissue engineering applications," *RSC Advances*, vol. 8, no. 56, pp. 31911–31923, 2018.

[6] J. S. Fernandes, P. Gentile, R. A. Pires, R. L. Reis, and P. V. Hatton, "Multifunctional bioactive glass and glass-ceramic biomaterials with antibacterial properties for repair and regeneration of bone tissue," *Acta Biomaterialia*, vol. 59, pp. 2–11, 2017.

[7] G. J. Lai, K. T. Shalumon, S. H. Chen, and J. P. Chen, "Composite chitosan/silk fibroin nanofibers for modulation of osteogenic differentiation and proliferation of human mesenchymal stem cells," *Carbohydrate Polymers*, vol. 111, pp. 288–297, 2014.

[8] J. Zhang, J. N. Li, G. L. Jia et al., "Improving osteogenesis of PLGA/HA porous scaffolds based on dual delivery of BMP-2 and IGF-1viaa polydopamine coating," *RSC Advances*, vol. 7, no. 89, pp. 56732–56742, 2017.

[9] P. M. Liu, L. Sun, P. Y. Liu et al., "Surface modification of porous PLGA scaffolds with plasma for preventing dimensional shrinkage and promoting scaffold-cell/tissue interactions," *Journal of Materials Chemistry B*, vol. 6, no. 46, pp. 7605–7613, 2018.

[10] T. L. Gao, W. W. Cui, Z. L. Wang et al., "Photo-immobilization of bone morphogenic protein 2 on PLGA/HA nanocomposites to enhance the osteogenesis of adipose-derived stem cells," *RSC Advances*, vol. 6, no. 24, pp. 20202–20210, 2016.

[11] G. Ciofani, L. Ricotti, A. Menciassi, and V. Mattoli, "Preparation, characterization and in vitro testing of poly(lactic-co-glycolic) acid/barium titanate nanoparticle composites for enhanced cellular proliferation," *Biomedical Microdevices*, vol. 13, no. 2, pp. 255–266, 2011.

[12] W. L. Gao, B. Feng, Y. X. Ni, Y. L. Yang, X. O. Lu, and J. Weng, "Protein adsorption and biomimetic mineralization behaviors of PLL-DNA multilayered films assembled onto titanium," *Applied Surface Science*, vol. 257, no. 2, pp. 538–546, 2010.

[13] Y. L. Miao, R. R. Yang, D. Y. B. Deng, and L. M. Zhang, "Poly(L-lysine) modified zein nanofibrous membranes as efficient scaffold for adhesion, proliferation, and differentiation of neural stem cells," *RSC Advances*, vol. 7, no. 29, pp. 17711–17719, 2017.

[14] Y. Yuan, X. D. Shi, Z. H. Gan, and F. S. Wang, "Modification of porous PLGA microspheres by poly-L-lysine for use as tissue engineering scaffolds," *Colloids and Surfaces B: Biointerfaces*, vol. 161, pp. 162–168, 2018.

[15] Y. Luo, H. Shen, Y. X. Fang et al., "Enhanced proliferation and osteogenic differentiation of mesenchymal stem cells on graphene oxide-incorporated electrospun poly(lactic-co-glycolic acid) nanofibrous mats," *ACS Applied Materials & Interfaces*, vol. 7, no. 11, pp. 6331–6339, 2015.

[16] W.-G. La, M.-J. Jung, J.-K. Yoon et al., "Bone morphogenetic protein-2 for bone regeneration - dose reduction through graphene oxide-based delivery," *Carbon*, vol. 78, pp. 428–438, 2014.

[17] S. C. Thickett, E. Hamilton, G. Yogeswaran, P. B. Zetterlund, B. L. Farrugia, and M. S. Lord, "Enhanced osteogenic differentiation of human fetal cartilage rudiment cells on graphene oxide-PLGA hybrid microparticles," *Journal of functional biomaterials.*, vol. 10, no. 3, p. 33, 2019.

[18] Z. P. Qi, W. L. Guo, S. Zheng et al., "Enhancement of neural stem cell survival, proliferation and differentiation by IGF-1 delivery in graphene oxide-incorporated PLGA electrospun nanofibrous mats," *RSC Advances*, vol. 9, no. 15, pp. 8315–8325, 2019.

[19] Z. Y. Wang, H. Shen, S. J. Song et al., "Graphene oxide incorporated PLGA nanofibrous scaffold for solid phase gene delivery into mesenchymal stem cells," *Journal of Nanoscience and Nanotechnology*, vol. 18, no. 4, pp. 2286–2293, 2018.

[20] W. Qian, X. D. Hu, W. F. He et al., "Polydimethylsiloxane incorporated with reduced graphene oxide (rGO) sheets for wound dressing application: preparation and characterization," *Colloids and Surfaces B: Biointerfaces*, vol. 166, pp. 61–71, 2018.

[21] H. W. Ji, H. J. Sun, and X. G. Qu, "Antibacterial applications of graphene-based nanomaterials: recent achievements and challenges," *Advanced Drug Delivery Reviews*, vol. 105, Part B, pp. 176–189, 2016.

[22] C. Fu, H. T. Bai, Q. Hu, T. L. Gao, and Y. S. Bai, "Enhanced proliferation and osteogenic differentiation of MC3T3-E1 pre-osteoblasts on graphene oxide-impregnated PLGA-gelatin nanocomposite fibrous membranes," *RSC Advances*, vol. 7, no. 15, pp. 8886–8897, 2017.

[23] D. M. K. Ciombor and R. K. Aaron, "The role of electrical stimulation in bone repair," *Foot and Ankle Clinics*, vol. 10, no. 4, pp. 579–593, 2005.

[24] S. Ebrahim, B. Mollon, S. Bance, J. Busse, and M. Bhandari, "Low-intensity pulsed ultrasonography versus electrical stimulation for fracture healing: a systematic review and network meta-analysis," *Canadian Journal of Surgery*, vol. 57, no. 3, pp. E105–E118, 2014.

[25] S. Sun, I. Titushkin, and M. Cho, "Regulation of mesenchymal stem cell adhesion and orientation in 3D collagen scaffold by electrical stimulus," *Bioelectrochemistry*, vol. 69, no. 2, pp. 133–141, 2006.

[26] I. S. Kim, J. K. Song, Y. M. Song et al., "Novel effect of biphasic electric current on in vitro osteogenesis and cytokine production in human mesenchymal stromal cells," *Tissue Engineering Parts A*, vol. 15, no. 9, pp. 2411–2422, 2009.

[27] Q. W. Xu, L. Jin, C. Li, S. Kuddannayai, and Y. L. Zhang, "The effect of electrical stimulation on cortical cells in 3D nanofibrous scaffolds," *RSC Advances*, vol. 8, no. 20, pp. 11027–11035, 2018.

[28] W. Zhu, T. Ye, S. J. Lee et al., "Enhanced neural stem cell functions in conductive annealed carbon nanofibrous scaffolds with electrical stimulation," *Nanomedicine: Nanotechnology, Biology and Medicine*, vol. 14, no. 7, pp. 2485–2494, 2018.

[29] R. L. Qi, X. Cao, M. Shen, R. Guo, J. Yu, and X. Shi, "Biocompatibility of electrospun halloysite nanotube-doped poly (lactic-co-glycolic acid) composite nanofibers," *Journal of Biomaterials Science, Polymer Edition*, vol. 23, no. 1-4, pp. 299–313, 2012.

[30] M. J. Dalby, D. McCloy, M. Robertson, C. D. W. Wilkinson, and R. O. C. Oreffo, "Osteoprogenitor response to defined topographies with nanoscale depths," *Biomaterials*, vol. 27, no. 8, pp. 1306–1315, 2006.

[31] G. J. Hickman, A. Rai, D. J. Boocock, R. C. Rees, and C. C. Perry, "Fabrication, characterisation and performance of hydrophilic and super-hydrophilic silica as cell culture surfaces," *Journal of Materials Chemistry*, vol. 22, no. 24, pp. 12141–12148, 2012.

[32] X. D. Shi, L. Sun, J. Jiang, X. L. Zhang, W. J. Ding, and Z. H. Gan, "Biodegradable polymeric microcarriers with controllable porous structure for tissue engineering," *Macromolecular Bioscience*, vol. 9, no. 12, pp. 1211–1218, 2009.

[33] Z. H. Zheng, L. Zhang, L. J. Kong, A. J. Wang, Y. D. Gong, and X. F. Zhang, "The behavior of MC3T3-E1 cells on chitosan/-poly-L-lysine composite films: effect of nanotopography, surface chemistry, and wettability," *Journal of Biomedical Materials Research Part A*, vol. 89A, no. 2, pp. 453–465, 2009.

[34] P. Arriagada, H. Palza, P. Palma, M. Flores, and P. Caviedes, "Poly(lactic acid) composites based on graphene oxide particles with antibacterial behavior enhanced by electrical stimulus and biocompatibility," *Journal of Biomedical Materials Research Part A*, vol. 106, no. 4, pp. 1051–1060, 2018.

[35] M. Patila, I. V. Pavlidis, A. Kouloumpis et al., "Graphene oxide derivatives with variable alkyl chain length and terminal functional groups as supports for stabilization of cytochrome c," *International Journal of Biological Macromolecules*, vol. 84, pp. 227–235, 2016.

[36] B. Cai, K. B. Hu, C. M. Li, J. Jin, and Y. X. Hu, "Bovine serum albumin bioconjugated graphene oxide: red blood cell adhesion and hemolysis studied by QCM-D," *Applied Surface Science*, vol. 356, pp. 844–851, 2015.

[37] H. Shen, M. Liu, H. He et al., "PEGylated graphene oxide-mediated protein delivery for cell function regulation," *ACS Applied Materials & Interfaces*, vol. 4, no. 11, pp. 6317–6323, 2012.

[38] C. T. Barrett and J. F. Barrett, "Antibacterials: are the new entries enough to deal with the emerging resistance problems?," *Current Opinion in Biotechnology*, vol. 14, no. 6, pp. 621–626, 2003.

[39] I. E. Mejías Carpio, C. M. Santos, X. Wei, and D. F. Rodrigues, "Toxicity of a polymer-graphene oxide composite against bacterial planktonic cells, biofilms, and mammalian cells," *Nanoscale*, vol. 4, no. 15, pp. 4746–4756, 2012.

[40] D. Alkekhia and A. Shukla, "Effect of poly-L-lysine molecular weight on antibacterial activity in polyelectrolyte multilayer assemblies," *Abstracts of Papers of the American Chemical Society*, vol. 256, 2018.

[41] Z. P. Qi, P. Xia, S. Pan et al., "Combined treatment with electrical stimulation and insulin-like growth factor-1 promotes bone regeneration in vitro," *PLoS One*, vol. 13, no. 5, article e0197006, 2018.

[42] K. Qiao, S. Guo, Y. Zheng et al., "Effects of graphene on the structure, properties, electro-response behaviors of GO/PAA composite hydrogels and influence of electro-mechanical coupling on BMSC differentiation," *Materials Science & Engineering, C: Materials for Biological Applications*, vol. 93, pp. 853–863, 2018.

[43] K. W. Chun, H. S. Yoo, J. J. Yoon, and T. G. Park, "Biodegradable PLGA microcarriers for injectable delivery of chondrocytes: effect of surface modification on cell attachment and function," *Biotechnology Progress*, vol. 20, no. 6, pp. 1797–1801, 2004.

[44] P. Li, J. W. Xu, L. Z. Liu, Y. N. Zhang, M. L. Liu, and Y. B. Fan, "Promoting proliferation and differentiation of pre-osteoblasts MC3T3-E1 cells under combined mechanical and electrical stimulation," *Journal of Biomedical Nanotechnology*, vol. 15, no. 5, pp. 921–929, 2019.

[45] F. Y. Qi, Y. Q. Wang, T. Ma et al., "Electrical regulation of olfactory ensheathing cells using conductive polypyrrole/chitosan polymers," *Biomaterials*, vol. 34, no. 7, pp. 1799–1809, 2013.

[46] M. R. Love, S. Palee, S. C. Chattipakorn, and N. Chattipakorn, "Effects of electrical stimulation on cell proliferation and apoptosis," *Journal of Cellular Physiology*, vol. 233, no. 3, pp. 1860–1876, 2018.

[47] L. Munaron, S. Antoniotti, and D. Lovisolo, "Intracellular calcium signals and control of cell proliferation: how many mechanisms?," *Journal of Cellular and Molecular Medicine*, vol. 8, no. 2, pp. 161–168, 2004.

[48] H. Y. Zhou, Y. Ohnuma, H. Takita, R. Fujisawa, M. Mizuno, and Y. Kuboki, "Effects of a bone lysine-rich 18 kDa protein on osteoblast-like MC3T3-E1 cells," *Biochemical and Biophysical Research Communications*, vol. 186, no. 3, pp. 1288–1293, 1992.

[49] L. J. Zhang, S. Ramsaywack, H. Fenniri, and T. J. Webster, "Enhanced osteoblast adhesion on self-assembled nanostructured hydrogel scaffolds," *Tissue Engineering Part A*, vol. 14, no. 8, pp. 1353–1364, 2008.

[50] D. Y. Kim, H. Park, and K. Y. Lee, "Effect of the mechanical properties of cell-interactive hydrogels on a control of cell phenotype," *PolymerKorea*, vol. 39, no. 3, pp. 412–417, 2015.

[51] A. Parandakh, A. Anbarlou, M. Tafazzoli-Shadpour, A. Ardeshirylajimi, and M. M. Khani, "Substrate topography interacts with substrate stiffness and culture time to regulate mechanical properties and smooth muscle differentiation of mesenchymal stem cells," *Colloids and Surfaces B: Biointerfaces*, vol. 173, pp. 194–201, 2019.

[52] S. Kang, J. B. Park, T.-J. Lee et al., "Covalent conjugation of mechanically stiff graphene oxide flakes to three- dimensional collagen scaffolds for osteogenic differentiation of human mesenchymal stem cells," *Carbon*, vol. 83, pp. 162–172, 2015.

[53] R. Ravichandran, J. R. Venugopal, S. Sundarrajan, S. Mukherjee, and S. Ramakrishna, "Precipitation of nanohydroxyapatite on PLLA/PBLG/collagen nanofibrous structures for the differentiation of adipose derived stem cells to osteogenic lineage," *Biomaterials*, vol. 33, no. 3, pp. 846–855, 2012.

[54] G. X. Sun, L. J. Wang, C. Xiang, and K. R. Qin, "A dynamic model for intracellular calcium response in fibroblasts induced by electrical stimulation," *Mathematical Biosciences*, vol. 244, no. 1, pp. 47–57, 2013.

[55] L. L. Li, X. C. Shi, Z. L. Wang, Y. Wang, Z. X. Jiao, and P. B. Zhang, "*In situ* polymerization of poly(γ-benzyl-l-glutamate) on mesoporous hydroxyapatite with high graft amounts for the direct fabrication of biodegradable cell microcarriers and their osteogenic induction," *Journal of Materials Chemistry B*, vol. 6, no. 20, pp. 3315–3330, 2018.

[56] M. O. Oftadeh, B. Bakhshandeh, M. M. Dehghan, and A. Khojasteh, "Sequential application of mineralized electroconductive scaffold and electrical stimulation for efficient osteogenesis," *Journal of Biomedical Materials Research Part A*, vol. 106, no. 5, pp. 1200–1210, 2018.